PROCEEDINGS OF SCIENCE

The ATLAS Transverse Momentum Trigger at the LHC

Allen I. Mincer* **(On behalf of the ATLAS Collaboration)**
New York University (US)
E-mail: allen.mincer@nyu.edu

The transverse momentum triggers of the ATLAS experiment at the CERN Large Hadron Collider (LHC) are designed to select collision events with non-interacting particles passing through the detector. Such events provide an interesting probe for new-physics interactions beyond the Standard Model, and also provide the basis for precise measurements of Standard Model parameters such as Higgs couplings. The transverse momentum used in the trigger system is calculated from calorimeter-based global energy sums and supplemented with information from the muon detection system. The trigger successfully operated during the first running period of the LHC. Starting in 2015 the LHC will produce collisions at higher energy and increased luminosity; improving on the trigger performance from the previous run period will be challenging.

The European Physical Society Conference on High Energy Physics
22-29 July 2015
Vienna, Austria

*Speaker.

PoS(EPS-HEP2015)269

1. Run I Trigger Algorithms

The goal of the ATLAS experiment [1] missing transverse momentum ($E_{\mathrm{T}}^{\mathrm{miss}}$) triggers [2, 3, 4] is to select events with an imbalance in the total measured momentum due to non-interacting particles which pass through the detector, in order to probe for new physics and perform precise measurements of Standard Model parameters.

LHC Run I triggers used the calorimeter-based global energy sums $E_{\mathrm{x}}^{\mathrm{miss}} = -\Sigma_i \sin\theta_i \cos\phi_i$, $E_{\mathrm{y}}^{\mathrm{miss}} = -\Sigma_i \sin\theta_i \sin\phi_i$, (both supplemented in some cases with muon measurements), and $E_{\mathrm{T}}^{\mathrm{miss}} = \sqrt{(E_{\mathrm{x}}^{\mathrm{miss}})^2 + (E_{\mathrm{y}}^{\mathrm{miss}})^2}$, where the sums are over all calorimeter cells (or cell-groupings) i, E_i is the energy measured in cell i, θ_i is the angle between the cell i position vector (measured from the center of the ATLAS detector) and the beam axis, and ϕ_i is the cell position angle from the horizontal in the plane transverse to the beam axis. The triggers select events for which $E_{\mathrm{T}}^{\mathrm{miss}}$ is above set threshold values. Transverse energy sum ($\Sigma E_T = \Sigma_i E_i \sin\theta_i$) triggers were used to select proton-proton events with large calorimeter energy, and to signal heavy-ion collisions.

In Run I, ATLAS used a three-level trigger system [5]. The lowest-level (L1) trigger used firmware on custom electronics to obtain coarse-grained sums over projective "trigger towers" ($\Delta\eta \times \Delta\phi \sim 0.2 \times 0.2$ for $|\eta| < 2.5$ and larger and less regular for larger η) to determine transverse momentum quantities. Energy resolution and zero suppression for trigger towers were about 1 GeV. This result was also used through 2011 for the next-higher (L2) trigger level.

The bulk of $E_{\mathrm{T}}^{\mathrm{miss}}$ triggers arise from fluctuations in the measurement of energy deposited in the calorimeter. Fluctuations increase at high luminosity, since multiple proton-proton interactions, in addition to any particular one of interest, occur in every bunch crossing. These deposit “pileup" energy in the calorimeter, both for the bunch-crossing in which they occur (“in-time pileup") and for later bunches (“out-of-time pileup"). LHC bunches come in trains, with sets of colliding bunches spaced by 50 ns (in most of LHC Run 1), separated by collisionless gaps. Bipolar calorimeter electronic signal shaping results in cancellation of the average of (but not of the fluctuations in) in-time and out-of-time pileup for bunches after the first few in a train.

In 2012, for which the average number of expected interactions per bunch crossing, μ, regularly exceeded 40, improvements were made to decrease the effects of pileup. L1 zero suppression took into account the η dependence of pileup. Some 2012 L1 $E_{\mathrm{T}}^{\mathrm{miss}}$ triggers omitted the first 3 bunches in a train. Also, an improved L2 algorithm was employed, using firmware modifications to supply the sum over (typically 128) cells in front-end boards (FEBs). Cells with energy less than three times the noise standard deviation, σ_N, and noisy cells were suppressed from the sum.

The access to the full data and additional CPU time available at the third (EF) trigger level allowed use of the full ~188,000 calorimeter-cell granularity. The algorithm used through 2011 omitted from the sum any cell i with energy $E_i < 3\sigma_N$. In order to more closely mimic the offline algorithm [6, 7, 8], the 2012 EF algorithm omitted cells with $|E_i| < 2\sigma_N$. The trigger was protected from large fluctuations by rejecting cells with $E_i < -5\sigma_N$. In 2012, σ_N included average pileup effects for the expected μ.

An additional EF-level algorithm, more like the offline one, was also run for some triggers in 2012. This cluster algorithm used seed cells with $|E_i| > 4\sigma_N$, surrounding cells with $|E_i| > 2\sigma_N$, and all immediate neighbor cells. It also included local hadronic calibration [7], though not the full object calibration of the offline algorithms.

The $E_{\mathrm{T}}^{\mathrm{miss}}$ significance (XS) triggers were designed to select events whose $E_{\mathrm{T}}^{\mathrm{miss}}$ is large compared with what is expected from measurement fluctuations. The width of $E_{\mathrm{x}}^{\mathrm{miss}}$ and $E_{\mathrm{y}}^{\mathrm{miss}}$ distributions for events collected with a random trigger on colliding bunches (the bulk of which do not have real $E_{\mathrm{T}}^{\mathrm{miss}}$) are used to quantify the $E_{\mathrm{T}}^{\mathrm{miss}}$ fluctuations. As seen in the example in Figure 1 (left), for a narrow ΣE_T interval these distributions are well-fit by Gaussians. As can be seen in Figure 1 (right), the standard deviations determined from these fits are in turn well-modeled by assuming a dependence on only ΣE_T in the event, of the form $\sigma = a + b\sqrt{\Sigma E_T}$. With a and b extracted from fits like the ones in Figure 1, XS of an event with measured value of $E_{\mathrm{T}}^{\mathrm{miss}}$ and ΣE_T is then defined as $E_{\mathrm{T}}^{\mathrm{miss}}/\sigma$. Because of rate limitations, only some fraction of events passing these triggers (as determined by a "prescale factor") are retained. These triggers were useful in selecting a sample of events with $E_{\mathrm{T}}^{\mathrm{miss}}$ values below the rate-limited thresholds of $E_{\mathrm{T}}^{\mathrm{miss}}$ triggers. By their design, the rates of these triggers are more stable than $E_{\mathrm{T}}^{\mathrm{miss}}$ triggers with changes in μ.

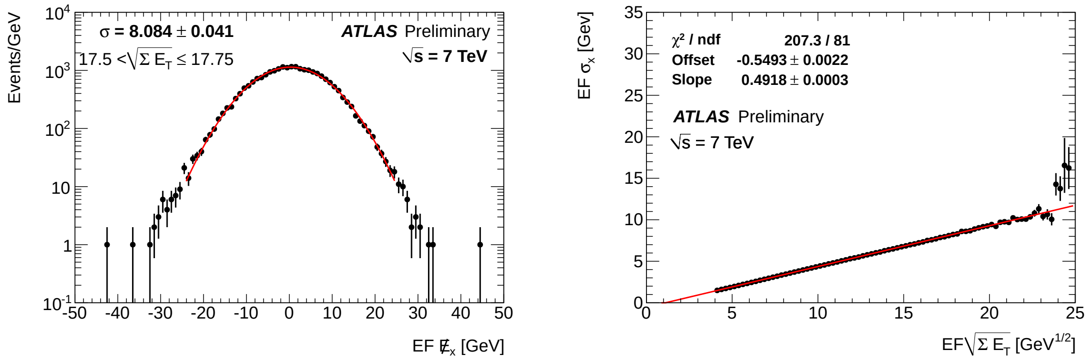

Figure 1: EF level calorimeter cell-sum algorithm determination of $E_{\mathrm{x}}^{\mathrm{miss}}$ for events triggered on random bunch crossings [4]. Left: $E_{\mathrm{x}}^{\mathrm{miss}}$ for events with $17.5 < \sqrt{\Sigma E_T} < 17.75$. The red line is a Gaussian fit to the distribution. Right: Standard deviation of $E_{\mathrm{x}}^{\mathrm{miss}}$ as a function of event ΣE_T. Each point and its error comes from a fit like the one shown in the left figure. Parameters given are for the linear fit (red line).

2. Performance of Run I Trigger Algorithms

Figure 2 (left) shows $E_{\mathrm{T}}^{\mathrm{miss}}$ distributions for events collected with a random trigger on colliding bunches. Pileup causes the $E_{\mathrm{T}}^{\mathrm{miss}}$ values (and therefore trigger rates) to rise sharply with μ. As LHC luminosity goes up, the trigger threshold or prescale factor must be therefore be increased. Figure 3 compares the measured efficiency of the lowest threshold unprescaled 2011 trigger for candidate $W \to \mu\nu$ events collected at 7 TeV with that predicted by simulation. Agreement between data and simulation is excellent.

Figure 2 (right) shows that, unlike $E_{\mathrm{T}}^{\mathrm{miss}}$, the XS distributions remain very similar even when μ increases by a factor of 4. The differences in the tail arise from other sources of $E_{\mathrm{T}}^{\mathrm{miss}}$, such as mis-measurement of jet energy in QCD 2-jet events, not captured in the ΣE_{T} parametrization.

Figure 4 compares the offline determination of $E_{\mathrm{T}}^{\mathrm{miss}}$ with that of various trigger algorithms used in 2012 for events collected with a random trigger on colliding bunches. The FEB algorithm, used at L2 in 2012, is much better correlated with the offline one than the trigger tower algorithm which was used at L2 in 2011 but only at L1 in 2012. The 2012 EF-level cluster algorithm is much better correlated with the offline one than the 2011 EF cell-sum algorithm.

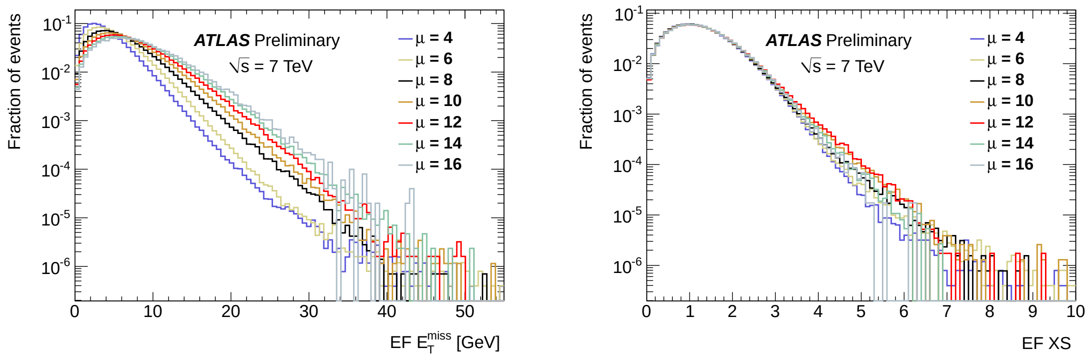

Figure 2: EF level $E_{\mathrm{T}}^{\mathrm{miss}}$ (left) and XS (right) for various values of μ for events collected with a random trigger on colliding bunches [4]. For the XS plots, events identified offline as having calorimeter noise bursts or badly measured jets were removed from the data samples used.

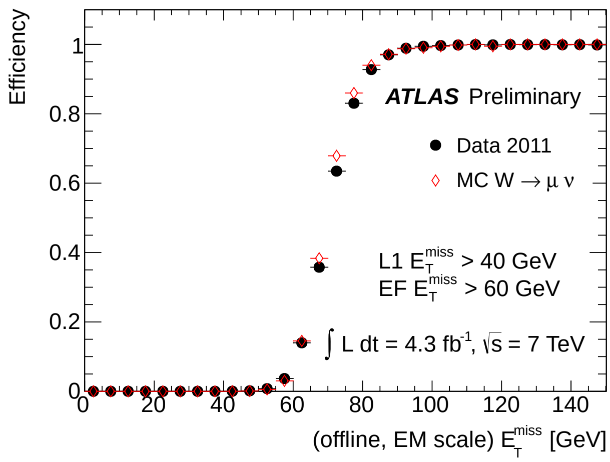

Figure 3: Comparison of measured and simulated efficiency of an $E_{\mathrm{T}}^{\mathrm{miss}}$ trigger with a threshold of about 40 GeV at L1 and 60 GeV at EF level for $W \to \mu\nu$ candidate events [4]. The data sample was selected with a trigger requiring a muon candidate. Non-W background was reduced by including offline cuts on the primary vertex and the W transverse mass. Events are simulated with the ATLAS simulation framework [9] using the PYTHIA6 [10] program and the the ATLAS MC11 AUET2B MRST LO** tune [11]. The GEANT4 [12] software package is used to simulate the passage of particles through the ATLAS detector. The transverse momentum of muons is not included in these determinations of $E_{\mathrm{T}}^{\mathrm{miss}}$. Because it involves a sum over the full calorimeter, the efficiency behavior may vary significantly for different event samples.

3. Towards Run II

The expected luminosity and energy increase of LHC Run II will result in increased pileup and much larger trigger rates. The $E_{\mathrm{T}}^{\mathrm{miss}}$ trigger rates can be controlled by increasing thresholds, while σ automatically gets larger for XS triggers, but these both result in reduced efficiency for events with true $E_{\mathrm{T}}^{\mathrm{miss}}$. This motivated a focus on event-by-event subtraction of pileup energy.

The introduction of an L1 topological processor makes possible a new algorithm that corrects the trigger-tower $E_{\mathrm{T}}^{\mathrm{miss}}$ with weighted sums of the transverse momenta p_{T} of proto-jets, built from energy depositions in specific regions of interest. The weight dependence on proto-jet η and p_{T},

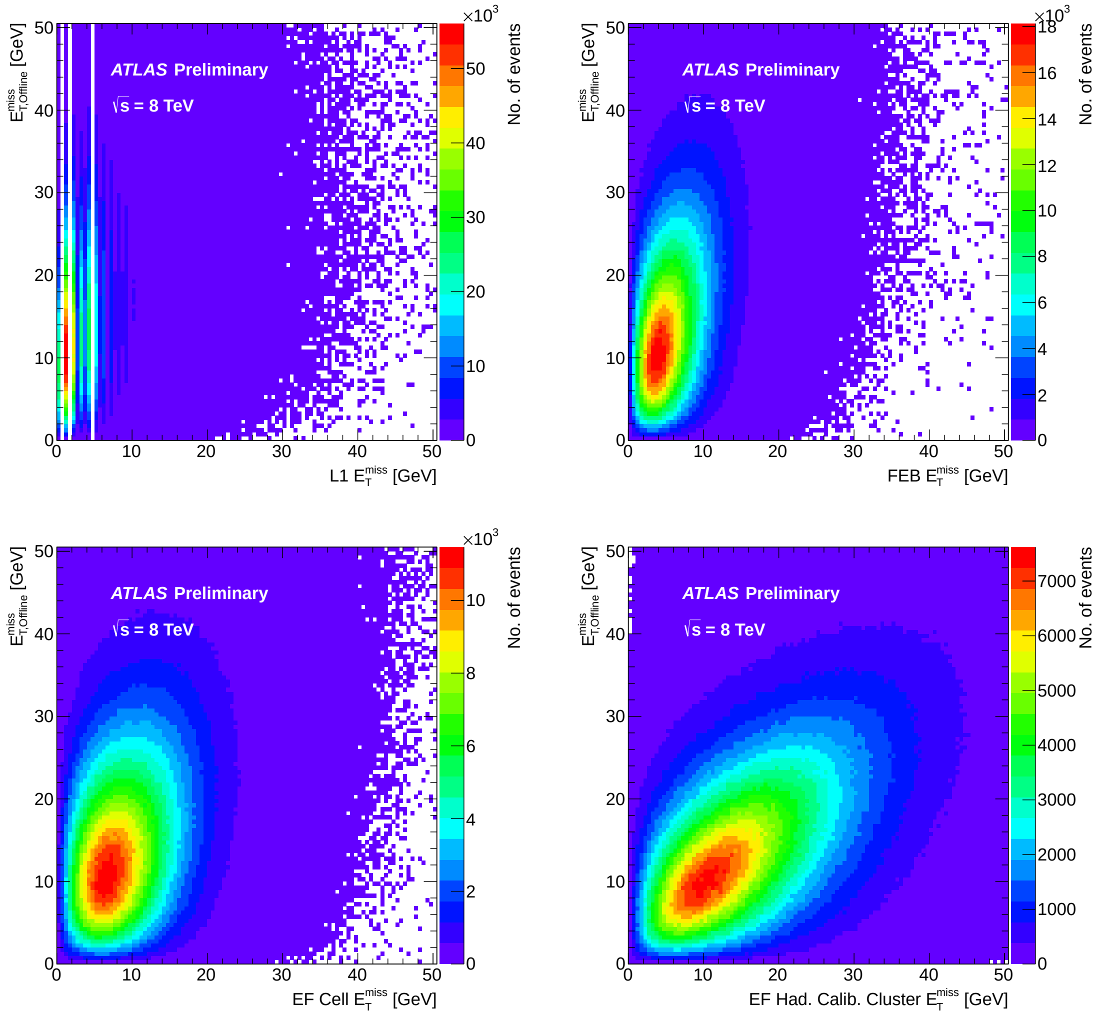

Figure 4: The missing transverse momentum of events collected in 2012 with a random trigger on crossing bunches as determined with the default offline algorithm versus values obtained with the 2012 L1 trigger-tower algorithm (similar to what was used also at L2 in 2011, top left), the 2012 L2 FEB algorithm (top right), the 2012 EF cell-sum algorithm (bottom left), and the EF-level cluster algorithm including correction for the hadronic energy scale (bottom right). The white stripes parallel to the y-axis in the top left plot are a consequence of the 1 GeV resolution on $E_{\mathrm{x}}^{\mathrm{miss}}$ and $E_{\mathrm{y}}^{\mathrm{miss}}$ which are added in quadrature to obtain L1 $E_{\mathrm{T}}^{\mathrm{miss}}$.

obtained using a Kalman filter, are shown in Figure 5 (left). The weights, w_i, are determined from simulated events with real $E_{\mathrm{T}}^{\mathrm{miss}}$ and severe ($\mu = 80$) pile-up by minimizing the difference of the true $E_{\mathrm{T}}^{\mathrm{miss}}$ in the event and the corrected sum $\vec{E}_{\mathrm{T}}^{\mathrm{miss\,L1}} - \Sigma_i w_i \vec{p}_{\mathrm{T}}^{\,jet\,i}$. Energy contributions from the forward region are weighted down to subtract pile-up, whereas central jets are weighted up to apply an ad-hoc calibration. The w_i have only a subleading dependence on the underlying physics sample, as the main correction comes from the energy depositions from pile-up collisions. Figure 5 (right) compares the expected efficiency of the L1 trigger-tower and the topological algorithms for simulated $ZH \rightarrow \nu\nu bb$ events. Efficiency improvement is clearly seen in this figure.

In Run II, the L2 and EF trigger levels are replaced by a single HLT level with full calorimeter

PoS(EPS-HEP2015)269

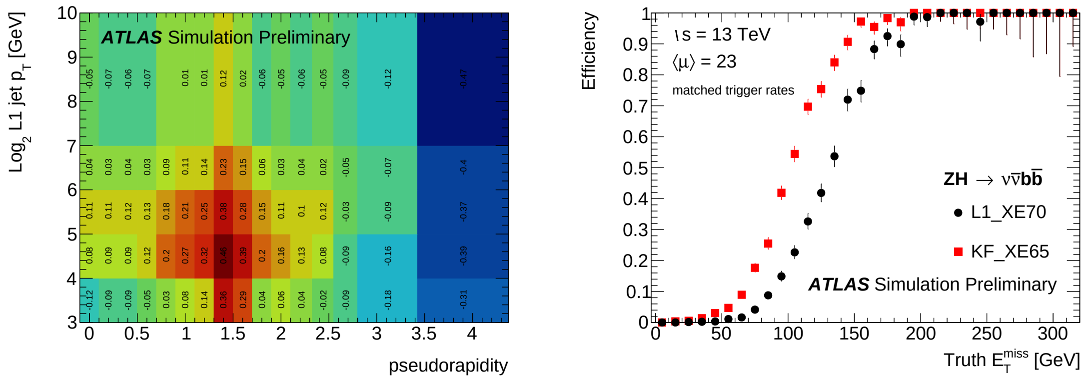

Figure 5: Left: The look-up-table of the L1 topological algorithm. Right: Efficiency of the corrected versus the original L1 E_T^{miss} for $ZH \to \nu\nu bb$ events simulated at 13 TeV with $\mu = 23$. Algorithm thresholds are set so that the two give the same total trigger rate, as estimated from simulated events without any real E_T^{miss}.

cell information and EF-quality muons. Algorithms designed to be less sensitive to pileup are being tested with early 13 TeV data; these include an algorithm that subtracts the average η-dependent pileup from calorimeter clusters, an algorithm that performs an event-by-event fit with E_T^{miss} from pileup constrained to be zero, and an algorithm that calculates E_T^{miss} from the jet p_T vector sum.

References

[1] ATLAS Collaboration, *The ATLAS Experiment at the CERN Large Hadron Collider*, *JINST* **3** (2008) S08003.

[2] D. Casadei et. al., *The implementation of the ATLAS missing* E_T *triggers for the initial LHC operation*, *ATL-DAQ-PUB-2011-001* (2011), http://cdsweb.cern.ch/record/1331180.

[3] ATLAS Collaboration, *Performance of the ATLAS transverse energy triggers with initial LHC runs at* $\sqrt{s} = 7$ *TeV*, *ATL-CONF-2011-072* (2011), http://cdsweb.cern.ch/record/1351836.

[4] ATLAS Collaboration, *The ATLAS transverse-momentum trigger performance at the LHC in 2011*, *ATL-CONF-2014-002* (2014), http://cdsweb.cern.ch/record/1647616.

[5] ATLAS Collaboration, *Performance of the ATLAS Trigger System in 2010*, *Eur. Phys. J.* **C72** (2012) 1849.

[6] ATLAS Collaboration, *Performance of missing transverse momentum reconstruction in proton-proton collisions at 7 TeV in ATLAS*, *Eur. Phys. J.* **C72** (2012) 1844.

[7] ATLAS Collaboration, *Local Hadronic Calbration*, *ATL-LARG-PUB-2009-001-2* (2009), http://cdsweb.cern.ch/record/1112035.

[8] ATLAS Collaboration, *Jet energy measurement with the ATLAS detector in proton-proton collisions at 7 TeV*, *Eur. Phys. J.* **C73** (2013) 2304.

[9] ATLAS Collaboration, *The ATLAS simulation infrastructure*, *Eur. Phys. J.* **C70** (2010) 823.

[10] T. Sjöstrand, S. Mrenna, and P. Z. Skands, *PYTHIA 6.4 physics and manual*, *JHEP* **0605** (2006) 026.

[11] The ATLAS Collaboration, *ATLAS tunes for Pythia6 and Pythia8 for MC11*, *ATLAS-PHYS-PUB-2011-009* (2011), http://cdsweb.cern.ch/record/1363300.

[12] S. Agostinelli et al., *GEANT4: A simulation toolkit*, *Nucl. Instrum. Meth.* **A506** (2003) 250.